Validation and steady-state analysis of a power-law model of purine metabolism in man

Raul CURTO*, Eberhard O. VOIT†, Albert SORRIBAS‡ and Marta CASCANTE*§

*Departament de Bioquímica i Biología Molecular, Facultat de Químiques, Universitat de Barcelona, 08028 Barcelona, Catalunya, Spain, †Department of Biometry and Epidemiology, Medical University of South Carolina, Charleston, SC 29425-2503, U.S.A., and ‡Departament de Ciències Mèdiques Bàsiques, Facultat de Medecina, Universitat de Lleida, 25198 Lleida, Catalunya, Spain

The paper introduces a model of human purine metabolism *in situ*. Chosen from among several alternative system descriptions, the model is formulated as a Generalized Mass Action system within Biochemical Systems Theory and validated with analyses of steady-state and dynamic characteristics. Eigenvalue and sensitivity analyses indicate that the model has a stable and robust steady-state. The model quite accurately reproduces numerous biochemical and clinical observations in healthy subjects as well as in patients with disorders of purine metabolism. These results suggest that the model can be used to assess biochemical and clinical aspects of human purine metabolism. It provides a means of exploring effects of enzyme deficiencies and is a potential tool for identifying steps of the pathway that could be the target of therapeutical intervention. Numerous quantitative comparisons with data are given. The model can be used for biomathematical exploration of relationships between enzymic deficiencies and clinically manifested diseases.

INTRODUCTION

Purine nucleotides and deoxynucleotides are the building blocks of life-defining information and, in the form of ATP, provide the energy support for most organisms. The pathway responsible for the supply and recycling of nucleotides and deoxynucleotides is purine metabolism. This pathway consists of an almost closed system that converts the two incoming precursors, ribose 5-phosphate (R5P) and glutamine, into nucleotides and essentially one degradation product, uric acid.

Because of its central role in the control of nucleotide pools, purine metabolism is of great importance in the context of carcinogenesis and viral diseases. Several purine metabolites or their analogues have been found to provide a powerful pharmaceutical basis for the treatment of these diseases, and also of some immune disorders [1,2] and major depression [3]. These successes have suggested the anti-metabolite theory [2] and triggered extensive research efforts to pinpoint the roles of enzymes and modulators of purine metabolism.

Nevertheless, given the complexity of the pathway (see Scheme 1; all abbreviations are defined in Tables 1 and 2), it is not surprising that our understanding of its functioning is still limited [4]. A large body of biochemical results *in vitro* and *in vivo* is available, and these results are the *sine qua non* of any further analysis. However, the biochemical information alone is not sufficient. For instance, it is not clear why and how enzyme deficiencies lead to some types of mental retardation, or how one could best intervene therapeutically in disorders of purine metabolism. Biomathematical analysis can be a complementary tool that is able to integrate different types of biochemical and clinical findings.

Several approaches to modelling purine metabolism have been developed in recent years. Franco and Canela [5] designed one of the first kinetic models of purine metabolism based on data from different species and tissues, with the aim of demonstrating the usefulness of computer simulations of complex metabolic networks. Heinmets [6] modelled nucleic acid synthesis from nucleotides and deoxynucleotides, although their parameters were not based on experimental data. More recently, Bartel and Holzhütter [7] constructed a model based on rat liver as the reference system. The goal of the present paper goes beyond these earlier analyses. It is to analyse purine metabolism in the human body, to test the results against clinical observations, and to make predictions about the responses of patients with disorders of purine metabolism to alternative drug therapies.

The process of designing a reliable mathematical model began with a comprehensive comparative analysis of different modelling approaches. This analysis was executed over a time period of several years in an iterative manner. The models were set up mathematically, parameter values were estimated from experimental data (see [8] for more details), and the steady-state and dynamic features were analysed in comparison with biochemical and clinical data, as shown for example by Shiraishi and Savageau [9–13] for a different biochemical system. Discrepancies between models and data were used for targeted refinements in model structure and led to the next iteration in the model design process. This process led to two conclusions. First, we found that for our purposes the mathematical form of a Generalized Mass Action (GMA) system was best suited. Secondly, the resulting GMA model could be estimated almost entirely from experimental data, and analyses of stability and robustness suggested that the numerical model promised reliability.

The main purpose of the present paper is a demonstration that our model is able to reproduce large sets of features that were experimentally or clinically observed in animals and humans [14–29]. The consistency with the biochemical and clinical

Abbreviations used: GMA, Generalized Mass Action; BST, Biochemical Systems Theory; MCT, Metabolic Control Theory. Other abbreviations are given in Tables 1 and 2.

§ To whom correspondence should be addressed.

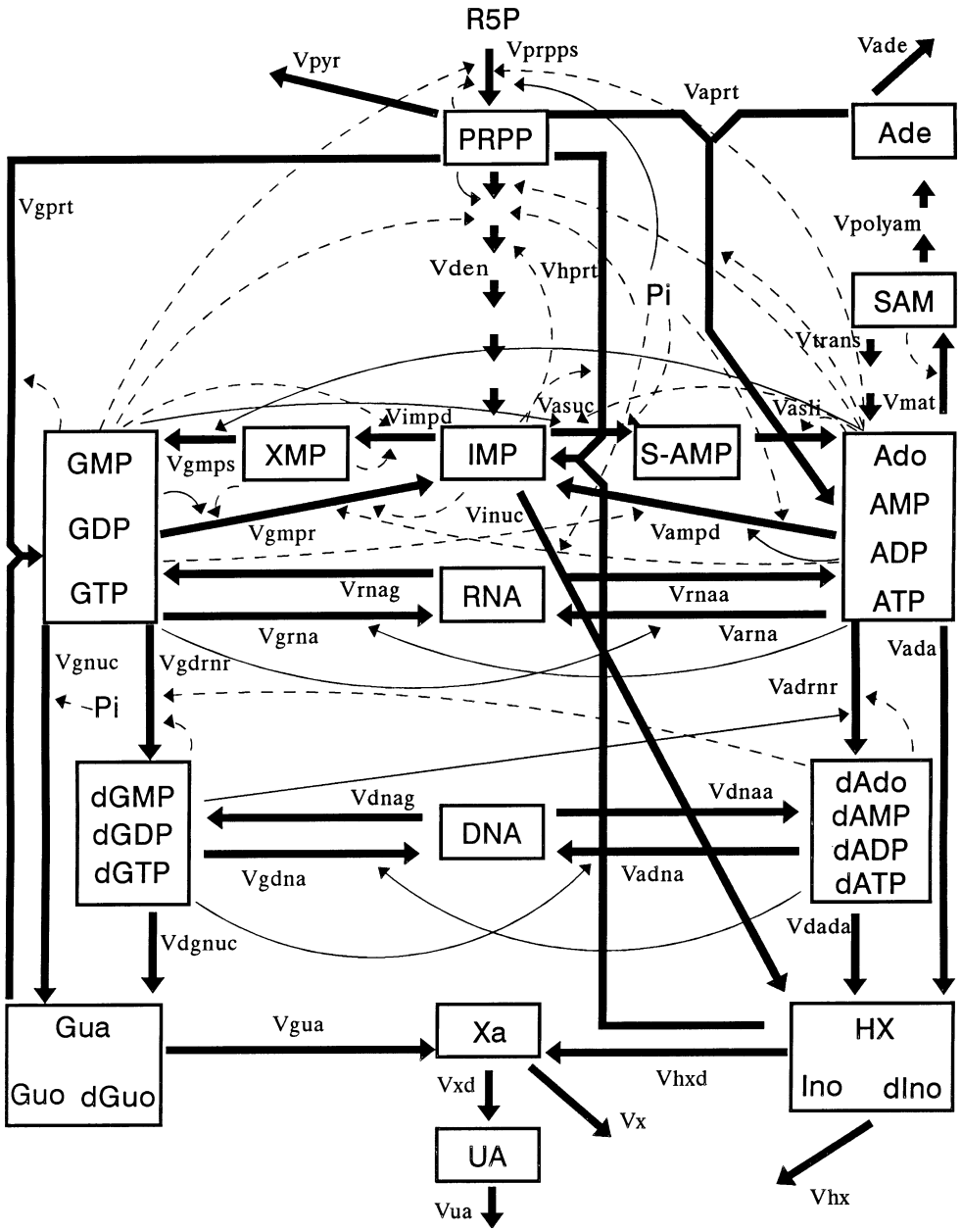

Scheme 1 Metabolic scheme of purine metabolism in man

Dependent variables are presented with boxes, independent variables (R5P and P_i) without. Fluxes are represented by straight heavy arrows and coded with mnemonic abbreviations. Regulatory signals and modulations of the pathway are represented by curved light arrows, with inhibitions given as dashed lines and activations as solid lines.

literature suggests that as yet untested model predictions might also be reliable and reasonably accurate. Such predictions address the dynamic and steady-state behaviour of the pathway after changes in dependent variables (shown here) and the derivation of cause- and- effect relationships between enzyme deficiencies and clinical symptoms.

METHODS

For the reasons mentioned above, the GMA approach within Biochemical Systems Theory (BST) [30] was chosen to model human purine metabolism. The tools of this modelling approach are explained in this section. They are divided into two subsections, those that concern model construction and the definition of the parameters, and those that are useful for the model analysis.

Model construction

The GMA model is constructed by defining a differential equation for each of the dependent variables of the model in the form

$$X_i = \sum_{j-1}^{r} c_{ij} v_j \qquad (1)$$

where r is the number of steps of the pathway. c_{ij} are the stoichiometric coefficients of step j of the synthesis or degradation

Table 1 Abbreviations for metabolites of purine metabolism (Scheme 1)

Abbreviation	Metabolite	Variable
PRPP	Phosphoribosylpyrophosphate	X_1
IMP	Inosine monophosphate	X_2
S-AMP	Adenylosuccinate	X_3
Ado	Adenosine	X_4
AMP	Adenosine monophosphate	
ADP	Adenosine diphosphate	
ATP	Adenosine triphosphate	
SAM	*S*-Adenosyl-L-methionine	X_5
Ade	Adenine	X_6
XMP	Xanthosine monophosphate	X_7
GMP	Guanosine monophosphate	X_8
GDP	Guanosine diphosphate	
GTP	Guanosine triphosphate	
dAdo	Deoxyadenosine	X_9
dAMP	Deoxyadenosine monophosphate	
dADP	Deoxyadenosine diphosphate	
dATP	Deoxyadenosine triphosphate	
dGMP	Deoxyguanosine monophosphate	X_{10}
dGDP	Deoxyguanosine diphosphate	
dGTP	Deoxyguanosine triphosphate	
RNA	Ribonucleic acid	X_{11}
DNA	Deoxyribonucleic acid	X_{12}
HX	Hypoxanthine	X_{13}
Ino	Inosine	
dIno	Deoxyinosine	
Xa	Xanthine	X_{14}
Gua	Guanine	X_{15}
Guo	Guanosine	
dGuo	Deoxyguanosine	
UA	Uric acid	X_{16}
R5P	Ribose 5-phosphate	X_{17}
P_i	Phosphate	X_{18}

of X_i, which can be positive if the reaction affects the synthesis of the metabolite or negative if the reaction affects the degradation of the metabolite. v_j is the rate law of step j in power-law form. In other words, the variation of each metabolite with respect to time is given by all processes synthesizing this metabolite minus all processes degrading the metabolite.

In BST, the kinetic rate law of each flux (v_j or v_{name}) in a given pathway is represented as a product of power-law functions of the form:

$$v_{\text{name}} = \alpha_{\text{name}} \prod_{i=1}^{n+m} X_i^{f_{\text{name}_i}} \tag{2}$$

In this formulation, n is the number of dependent variables in the model and m is the number of independent variables. All the kinetic orders are denoted by f followed by two subindices: first the abbreviated name of the reaction, and second the number of the variable that affects the rate of the reaction. Each kinetic order (f_{name_i}) quantifies the effect of the metabolite X_i on flux v_{name}. If it describes an inhibition, it has a negative value, and if it describes an activation or substrate effect, it has a positive value. They are similar to kinetic orders of elemental kinetics but may be non-integer. They are mathematically defined as:

$$f_{\text{name}_i} = \left(\frac{\partial v_{\text{name}}}{\partial X_i}\right)_0 \frac{X_{i_0}}{v_{\text{name}_0}} \tag{3}$$

The basis for the assignment of these values is explained in the following section, and their numerical values appear in Table 3.

The rate constant (α_{name}) represents the speed of process v_{name} [31]. It is computed as

$$\alpha_{\text{name}} = \frac{v_{\text{name}_0}}{\prod_{i=1}^{n+m} X_{i_0}^{f_{\text{name}_i}}} \tag{4}$$

Numerical values of rate constants appear in Table 4.

Model analysis

The quality of the model was tested with different analytical tools. Stability was assessed with the program ESSYNS [32] by computing the eigenvalues of the model. The criterion for local stability at a given steady state is that all eigenvalues have negative real parts. If the imaginary parts of some eigenvalues are different from 0, the system may exhibit oscillatory behaviour [13,33].

As a second criterion of quality, the robustness of the model at its steady state was evaluated. This was accomplished by computing the sensitivities of the concentrations with respect to the kinetic orders. In general, low sensitivities are an indication of a robust steady state, whereas high sensitivities often suggest that the pathway can be easily perturbed. In general, well-adapted biological systems are not expected to be highly sensitive to small changes in kinetic parameters and, consequently, low-parameter sensitivities can be used as a criterion of model validation [13,34]. The insensitivity of the kinetic parameter presents another advantage since it means that the behaviour of the model does not critically depend on very accurate estimates of this parameter [35]. The sensitivities of the model were computed with MATHEMATICA [36] as the normalized derivatives of metabolite concentrations with respect to kinetic orders [37,38]:

$$S(X_i, f_{\text{name}}) = \left(\frac{\partial X_i}{\partial f_{\text{name}}}\right)_0 \frac{f_{\text{name}_0}}{X_{i_0}} \tag{5}$$

This equation means that, if X_i is a metabolite and f_{name} is a kinetic order, the sensitivity ($S(X_i, f_{\text{name}}$) quantifies the effect of a change in the kinetic order f_{name} on the steady-state concentration of X_i.

In addition to parameter sensitivities, we characterized the steady state with profiles of logarithmic gains. These are the normalized derivatives of fluxes or concentrations with respect to an independent variable [37,39–41]. For example, if X_i is a dependent variable and X_j is an independent variable, the logarithmic gain $L(X_i, X_j)$ quantifies the effect of a change of the independent variable X_j on the steady-state concentration of X_i. The logarithmic gains were computed with the matrix method implemented in the program MIST [42] and with ESSYNS [32]. Mathematically logarithmic gains of concentrations and fluxes are defined as

$$L(X_i, X_j) = \left(\frac{\partial X_i}{\partial X_j}\right)_0 \frac{X_{j_0}}{X_{i_0}} \quad \text{and} \quad L(v_i, X_j) = \left(\frac{\partial v_i}{\partial X_j}\right)_0 \frac{X_{j_0}}{v_{i_0}} \tag{6}$$

Dynamic simulations and computations of steady states were also executed in MIST [42]. For numerical integration, MIST uses a third-order semi-implicit Runge–Kutta algorithm, and steady states are computed with a Newton method.

Simulations of enzyme deficiencies or superactivities were executed with two methods, either by modifying the value of α of the corresponding reactions or by introducing the enzymes as

Table 2 Abbreviations for enzymes of purine metabolism (Scheme 1)

Abbreviated flux	Enzyme abbreviation	Enzyme-catalysed reaction	EC number
V_{prpps}	PRPPS	Phosphoribosylpyrophosphate synthetase	2.7.6.1
V_{gprt}	HGPRT	Hypoxanthine–guanine phosphoribosyltransferase	2.4.2.8
V_{hprt}	HGPRT	Hypoxanthine–guanine phosphoribosyltransferase	2.4.2.8
V_{aprt}	APRT	Adenine phosphoribosyltransferase	2.4.2.7
V_{den}	ATASE	'*De novo* synthesis' (amidophosphoribosyltransferase)	2.4.2.14
V_{pyr}		'pyrimidine, tryptophan and histidine synthesis'	Several enzymes
V_{asuc}	ASUC	Adenylosuccinate synthetase	6.3.4.4
V_{asli}	ASLI	Adenylosuccinate lyase	4.3.2.2
V_{impd}	IMPD	IMP dehydrogenase	1.1.1.205
V_{gmps}	GMPS	GMP synthetase	6.3.4.1
V_{ampd}	AMPD	AMP deaminase	3.5.4.6
V_{gmpr}	GMPR	GMP reductase	1.6.6.8
V_{trans}	MT	'Transmethylation pathway' (protein *O*-methyltransferase)	2.1.1.24
V_{mat}	MAT	Methionine adenosyltransferase	2.5.1.6
V_{polyam}	SAMD	'Polyamine pathway' (*S*-adenosylmethionine decarboxylase)	4.1.1.50
V_{ade}		'Adenine oxidation' (xanthine dehydrogenase)	1.2.3.2 or 1.2.1.37
V_{inuc}	5NUC	5′-Nucleotidase	3.1.3.5
V_{gnuc}	5NUC	5′-Nucleotidase	3.1.3.5
V_{arna}	RNAP	RNA polymerase (from ATP)	2.7.7.6
V_{grna}	RNAP	RNA polymerase (from GTP)	2.7.7.6
V_{rnaa}	RNAN	RNases (to AMP)	Several enzymes
V_{rnag}	RNAN	RNases (to GMP)	Several enzymes
V_{dgnuc}	3NUC	5′(3′) Nucleotidase	3.1.3.31
V_{ada}	ADA	Adenosine deaminase	3.5.4.4
V_{dada}	ADA	Adenosine deaminase	3.5.4.4
V_{adrnr}	DRNR	Diribonucleotide reductase	1.17.4.1
V_{gdrnr}	DRNR	Diribonucleotide reductase	1.17.4.1
V_{gua}	GUA	Guanine hydrolase	3.5.4.3
V_{adna}	DNAP	DNA polymerase (from dATP)	2.7.7.7
V_{gdna}	DNAP	DNA polymerase (from dGTP)	2.7.7.7
V_{dnaa}	DNAN	DNases (to dAMP)	Several enzymes
V_{dnag}	DNAN	DNases (to dGMP)	Several enzymes
V_{hx}		'Hypoxanthine excretion'	Non-enzymic step
V_{hxd}	XD	Xanthine oxidase or xanthine dehydrogenase	1.2.3.2 or 1.2.1.37
V_{xd}	XD	Xanthine oxidase or xanthine dehydrogenase	1.2.3.2 or 1.2.1.37
V_{x}		'Xanthine excretion'	Non-enzymic step
V_{ua}		'Uric acid excretion'	Non-enzymic step

Table 3 Values of the kinetic orders, in alphabetical order

$f_{ada4} = 0.97$	$f_{ade6} = 0.55$	$f_{adrnr4} = 0.1$	$f_{adrnr9} = -0.3$
$f_{adrnr10} = 0.87$	$f_{ampd4} = 0.8$	$f_{ampd8} = -0.03$	$f_{ampd18} = -0.1$
$f_{aprt1} = 0.5$	$f_{aprt4} = -0.8$	$f_{aprt6} = 0.75$	$f_{asuc2} = 0.4$
$f_{asuc4} = -0.24$	$f_{asuc8} = 0.2$	$f_{asuc18} = -0.05$	$f_{asli3} = 0.99$
$f_{asli4} = -0.95$	$f_{dada9} = 1$	$f_{den1} = 2$	$f_{den2} = -0.06$
$f_{den4} = -0.25$	$f_{den8} = -0.2$	$f_{den18} = -0.08$	$f_{dgnuc10} = 1$
$f_{dnan12} = 1$	$f_{dnap9} = 0.42$	$f_{dnap10} = 0.33$	$f_{gdrnr8} = 0.4$
$f_{gdrnr9} = -1.2$	$f_{gdrnr10} = -0.39$	$f_{gmpr2} = -0.15$	$f_{gmpr4} = -0.07$
$f_{gmpr7} = -0.76$	$f_{gmpr8} = 0.7$	$f_{gmps4} = 0.12$	$f_{gmps7} = 0.16$
$f_{gnuc8} = 0.9$	$f_{gnuc18} = -0.34$	$f_{gprt1} = 1.2$	$f_{gprt8} = -1.2$
$f_{gprt15} = 0.42$	$f_{gua15} = 0.5$	$f_{hprt1} = 1.1$	$f_{hprt2} = -0.89$
$f_{hprt13} = 0.48$	$f_{hx13} = 1.12$	$f_{hxd13} = 0.65$	$f_{impd12} = 0.15$
$f_{impd7} = -0.09$	$f_{impd8} = -0.03$	$f_{inuc2} = 0.8$	$f_{inuc18} = -0.36$
$f_{mat4} = 0.2$	$f_{mat5} = -0.6$	$f_{polyam5} = 0.9$	$f_{prpps1} = -0.03$
$f_{prpps4} = -0.45$	$f_{prpps8} = -0.04$	$f_{prpps17} = 0.65$	$f_{prpps18} = 0.7$
$f_{pyr1} = 1.27$	$f_{rnan11} = 1$	$f_{rnap4} = 0.05$	$f_{rnap8} = 0.13$
$f_{trans5} = 0.33$	$f_{ua16} = 2.21$	$f_{x14} = 2.0$	$f_{xd14} = 0.55$

Table 4 Values of the rate constants, in alphabetical order

$\alpha_{ada} = 0.001062$	$\alpha_{ade} = 0.01$	$\alpha_{adna} = 3.2789$	$\alpha_{adrnr} = 0.0602$
$\alpha_{ampd} = 0.02688$	$\alpha_{aprt} = 233.8$	$\alpha_{arna} = 614.5$	$\alpha_{asuc} = 3.5932$
$\alpha_{asli} = 66544$	$\alpha_{dada} = 0.03333$	$\alpha_{den} = 5.2728$	$\alpha_{dgnuc} = 0.03333$
$\alpha_{dnaa} = 0.001938$	$\alpha_{dnag} = 0.001318$	$\alpha_{gdna} = 2.2296$	$\alpha_{gdrnr} = 0.1199$
$\alpha_{gmpr} = 0.3005$	$\alpha_{gmps} = 0.3738$	$\alpha_{gnuc} = 0.2511$	$\alpha_{gprt} = 361.69$
$\alpha_{grna} = 409.6$	$\alpha_{gua} = 0.4919$	$\alpha_{hprt} = 12.569$	$\alpha_{hx} = 0.003793$
$\alpha_{hxd} = 0.2754$	$\alpha_{impd} = 1.2823$	$\alpha_{inuc} = 0.9135$	$\alpha_{mat} = 7.2067$
$\alpha_{polyam} = 0.29$	$\alpha_{prpps} = 0.9$	$\alpha_{pyr} = 1.2951$	$\alpha_{rnaa} = 0.06923$
$\alpha_{rnag} = 0.04615$	$\alpha_{trans} = 8.8539$	$\alpha_{ua} = 0.00008744$	$\alpha_{x} = 0.0012$
$\alpha_{xd} = 0.949$			

new independent variables of the system and modifying the value of the independent variable. As is to be expected, both procedures yielded the same results.

It is noted that the GMA approach does not use flux aggregation, as the otherwise closely related S-system approach does. In GMA, the kinetic orders $f_{\mathrm{name}\,i}$ are strictly equivalent to the elasticity coefficients (ϵ) in Metabolic Control Theory (MCT). Also, the logarithmic gains $L(X_i, X_j)$ and $L(v_{\mathrm{name}}, X_j)$ are equivalent to the control coefficients. This equivalence facilitates the characterization of the control distribution among the enzymes of the pathway, and the understanding of our results to readers more familiar with MCT.

Table 5 Estimates of metabolite concentrations

Definitions of abbreviations are given in Table 1.

Variable	Concn. (μM)	Metabolite	Conc. (μM)	References
X_1	5	PRPP	5	43, 44
X_2	100	IMP	100	45
X_3	0.2	S-AMP	0.2	46
X_4	2500	Ado	0.5	47
		AMP	200	48–50
		ADP	400	
		ATP	1900	
X_5	4	SAM	4	51, 52
X_6	1	Ade	1	48, 49
X_7	25	XMP	25	50
X_8	400	GMP	25	48, 53, 54
		GDP	75	
		GTP	300	
X_9	6	dAdo	0.1	48
		dAMP	0.5	14, 55
		dADP	1.4	
		dATP	4	
X_{10}	3	dGMP	0.1	14, 55
		dGDP	0.5	
		dGTP	2.4	
X_{11}	28600	RNA	28600	56, 57
X_{12}	5160	DNA	5160	58
X_{13}	10	HX	6.9	15, 47
		Ino	3	48, 59
		dIno	0.1	
X_{14}	5	Xa	5	60, 61
X_{15}	5	Gua	0.5	48, 59
		Guo	4.4	
		dGuo	0.1	
X_{16}	100	UA	100	62
X_{17}	18	R5P	18	56
X_{18}	1400	P_i	1400	63, 64

In order to build the mathematical model required for Scheme 1, one needs to estimate all parameters of eqn. (2) (kinetic orders and rate constants) for the 37 reactions of the scheme.

Kinetic order values are estimated using eqn. (3), which requires steady-state values of the system (fluxes and concentrations). Metabolic concentrations identified from experimental data are summarized in Table 5 (see [8] for more details). The characterization of values for the fluxes is more complex, because there are few direct measurements of fluxes in the intact human body.

Our model contains 37 fluxes and 16 dependent variables (see Scheme 1). Consequently, taking into account steady-state constraints for the 16 dependent variables, 16 of the fluxes can be formulated as linear combinations of the remaining 21. In addition to these steady-state constraints, it is known that the ratio of adenine and guanine in nucleic acids is approximately 3:2. This fact allows us to formulate four more constraints between the fluxes in steady-state:

$$v_{\mathrm{arna}} = (3/2)\, v_{\mathrm{grna}}$$

$$v_{\mathrm{rnaa}} = (3/2)\, v_{\mathrm{rnag}}$$

$$v_{\mathrm{adna}} = (3/2)\, v_{\mathrm{gdna}}$$

$$v_{\mathrm{dnaa}} = (3/2)\, v_{\mathrm{dnag}}$$

While very helpful, these constraints are not sufficient for a complete kinetic characterization. Seventeen more flux estimates or constraints between fluxes are needed, and these have been extracted from experimental data. These flux constraints are presented in Table 6.

With these estimates and constraints, the system of equations has a unique solution for the flux values at steady state; this solution is presented in Table 7 (see [8] for more details).

The estimated values of fluxes and metabolite concentrations of the system in steady state can be used to estimate the kinetic orders of each reaction in Scheme 1. In cases where the substrate or modifier of the reaction is an aggregated pool, it is necessary to distinguish between the different metabolites that comprise the pool. This is accomplished with the second subindex of the corresponding kinetic order which is given as the abbreviated name of the metabolite instead of the number of the variable. In these cases, it is assumed that the aggregated pool concentration is the sum of concentrations of the individual components and that the equilibrium between them is rapidly achieved. With this assumption it can be mathematically demonstrated that the kinetic order with respect to the aggregated pool is the sum of all kinetic orders with respect to each individual component of the pool.

Kinetic orders of steps in Scheme 1 that represent linear chains of reactions ($v_{\mathrm{den}}, v_{\mathrm{polyam}}$, and v_{trans}) have been estimated to be equal to the kinetic orders of the first enzyme of the corresponding chain (ATASE, SAMD and MT respectively). This assumption is valid because in the three cases the first enzyme of the linear chain is irreversible and its velocity is not affected by any other intermediary metabolite of the chain. Under these particular circumstances the flux logarithmic gains of a linear chain correspond exactly to the kinetic orders of the first reaction. Moreover, once the linear chain is considered to be a single step in the whole model of Scheme 1, the flux logarithmic gains of the linear chain become the kinetic orders of this step.

When characterizing a complex system such as this, no single procedure is sufficient for all parameter estimations, and use of different procedures is required to characterize the full parameter set. The numerical values of the kinetic orders have been obtained using the following methods (see [8] for more details).

(1) For steps corresponding to enzyme-catalysed reactions that are well characterized *in vitro* by polynomial rate laws, we estimate the kinetic orders by partial differentiation of rate laws at the steady-state operating point, according to the definition given in eqn. (3). Results are given in Table 8.

(2) For some steps, we know the percentage of inhibition (or activation) of the rate law by a given metabolite. If metabolite X_i at concentration C μM inhibits (or activates) the V_j at $P\%$, one obtains the constraint:

$$C^{f_{ji}} = 1 - (\mathrm{or} +)\frac{P}{100}$$

From such constraints we estimated the values of the f_{ij}. Results are given in Table 9.

(3) In other cases the percentage inhibition (or activation) is unknown, but we know the change in kinetic parameters evoked by a given concentration of the modifier. In these cases, we substituted the kinetic parameters in the corresponding rate law and obtained the percentage change in the flux rate caused by a given concentration of the modifier. From this information, we estimated the kinetic order using method 2 (see Table 9).

(4) In two cases, the *in vivo* flux rates of a given step are known for different concentrations of the metabolite that influences this rate. Assuming that no other metabolites influence this rate, the value of such an f_{ij} is given as the slope of a plot of logarithm of the rate versus the logarithm of the metabolite concentration [see

Table 6 Experimentally based flux equations

Number	Equation	References
1	$v_{ua} \simeq 2.27\ \mu$mol/min per body weight	62
2	$v_{hxd} + v_{hprt} \simeq 4.90\ \mu$mol/min per body weight	61
3	$v_{hprt} \simeq 3 \times v_{hxd}$	23, 62
4	$v_{hprt} \simeq v_{gprt}$	19, 65
5	$v_{gdrnr} + v_{gnuc} \simeq 9 \times v_{gmpr}$	19, 66
6	$v_{asuc} \simeq 5 \times v_{impd}$	67, 68
7	$v_{aprt} \simeq 1\ \mu$mol/min per body weight	26
8	$\frac{v_{ada}}{v_{dada}} \simeq \frac{[Ado]}{[dAdo]} \simeq 10$	47
9	$\frac{v_{gnuc}}{v_{dgnuc}} \simeq \frac{[GMP]}{[dGMP]} \simeq 250$	The same assumption as in eqn. (8)
10	$v_{trans} \simeq 14\ \mu$mol/min per body weight	55
11	$v_{pyr} \simeq 10\ \mu$mol/min per body weight	Assuming that purine synthesis is of the same order as pyrimidine synthesis
12	$v_{ade} \simeq 0.01\ \mu$mol/min per body weight	27
13	$v_{hx} \simeq 0.05\ \mu$mol/min per body weight	28
14	$v_{x} \simeq 0.03\ \mu$mol/min per body weight	28
15	$v_{ampd} \simeq 3 \times v_{ada}$	69
16	$v_{adna} + v_{gdna} = 17\ \mu$mol/min per body weight	58
17	$v_{arna} + v_{grna} = 3300\ \mu$mol/min per body weight	70

Table 7 Steady-state flux rates in man

Variables are listed in alphabetical order. Units are μmol/min per body weight.

$v_{ada} = 2.1$	$v_{ade} = 0.01$	$v_{adna} = 10$	$v_{adrnr} = 0.2$
$v_{ampd} = 5.69$	$v_{aprt} = 1$	$v_{arna} = 1980$	$v_{asuc} = 8$
$v_{asli} = 8$	$v_{dada} = 0.2$	$v_{den} = 2.39$	$v_{dgnuc} = 0.1$
$v_{dnaa} = 10$	$v_{dnag} = 6.8$	$v_{gdna} = 6.8$	$v_{gdrnr} = 0.1$
$v_{gmpr} = 0.5$	$v_{gmps} = 1.6$	$v_{gnuc} = 4.7$	$v_{gprt} = 3.7$
$v_{grna} = 1320$	$v_{gua} = 1.1$	$v_{hprt} = 3.7$	$v_{hx} = 0.05$
$v_{hxd} = 1.23$	$v_{impd} = 1.6$	$v_{inuc} = 2.68$	$v_{mat} = 15$
$v_{polyam} = 1.01$	$v_{prpps} = 20.79$	$v_{pyr} = 10$	$v_{rnaa} = 1980$
$v_{rnag} = 1320$	$v_{trans} = 13.99$	$v_{ua} = 2.3$	$v_{x} = 0.03$
$v_{xd} = 2.3$			

eqn. (3)]. Using this method, we estimated f_{ade6} (with data from [101]) and f_{ua16} (with data from [102]).

(5) In three other cases, only two or three data points were available, but using the same method with *in vitro* data from [93], we obtained the values $f_{adrnr,dGTP} = 0.87$, $f_{gdrnr,dATP} = -1.2$ and $f_{gdrnr,dGTP} = -0.39$.

(6) In steps affected by only one metabolite, there are only two unknowns in the GMA rate law of the process [see eqn. (2)]: the α and f parameters. If we have the values of flux rate and concentration of the metabolite at two different steady states (the operating point and one other point), we can solve for the two unknowns in the system of two equations. Using this method we estimated the values of $f_{hx13} = 1.12$ and $f_{x14} = 2$. The values of two steady states for v_x, v_{hx}, [HX] and [Xa] had been collected from control subjects (operating point) and HGPRT-deficient patients in which $v_x = 0.27\ \mu$mol/min per body weight, $v_{hx} = 0.45\ \mu$mol/min per body weight, [Xa] = 15 μM and [HX] = 50 μM [29].

(7) Three kinetic orders represent steps catalysed by more than one enzyme (f_{pyrl}, f_{rnan11} and f_{dnan12}) and these could not be estimated with any of these methods because the necessary information was lacking. In these cases we used reasonable guesses: (i) the flux v_{pyr} is the flux of formation of pyrimidines, histidine and tryptophan. The most important of these fluxes is the pyrimidine formation, and this begins with the phosphoribosyltransferase step. Thus we used an average value of the effect of PRPP in the three phosphoribosyltransferases of the pathway, yielding $f_{pyrl} = 1.27$. Several enzymes hydrolyse nucleic acids to nucleotides and deoxynucleotides: 5′,3′-exonucleases, 3′,5′-exonucleases, endonucleases, H ribonuclease and other unspecific enzymes. For simplicity, we set the values of the corresponding kinetic orders as $f_{rnan11} = 1$ and $f_{dnan12} = 1$. We will demonstrate later that these parameter estimates are probably sufficient because changes in these parameters do not significantly affect the behaviour of the system (see sensitivities with respect to these kinetic orders in Figure 1).

Using these various methods, we estimated the complete set of kinetic orders with respect to the metabolites of the pathway (Scheme 1). The complete set of these kinetic orders is presented in Table 3.

To complete the estimation of GMA parameters, we need to compute the rate constants. This was accomplished with eqn. (4) for every reaction, using the values of fluxes in Table 7, the values of concentrations in Table 5, and the values of kinetic orders in Table 3 (see Table 4).

Finally, the GMA model representing purine metabolism in humans results from the mass-balance equations for the 16 dependent variables of the pathway, in which the rate laws of all reactions are in power-law form [eqn. (2)], and the kinetic orders and rate constants in these equations are substituted with the numerical values of Tables 3 and 4.

RESULTS

The tools developed within BST allow us to establish a complete characterization of a given model in terms of eigenvalues, sensitivities, logarithmic gains, the prediction of new steady

Table 8 Estimates of GMA kinetic orders, using method 1

Units for constants are μM.

Reaction	Kinetic equation	Kinetic parameters	Estimate	References
V_{prpps}	Michaelis–Menten	K_m (ATP) = 14 K_m (R5P) = 33	$f_{prpps,ATP} = 0.007$ $f_{prpps17} = 0.65$	71 56
V_{prpps}	Michaelis–Menten (apparent)	K_m (P_i) = 3300	$f_{prpps18} = 0.7$	72
V_{den}	Hill	K_m = 140–480 h = 2–3	f_{den1} = 1.6–2.3	21
V_{gprt}	Ordered sequence	$[PP_i] = 15$ $K_{PRPP} = 240$, $K_{Gua} = 4$ K_i (PP_i) = 2100, K_i (GMP) = 1.25	 $f_{gprt1} = 1.2$ $f_{gprt,GMP} = -1.2$ $f_{gprt,Gua} = 0.42$	73 74
V_{hprt}	Random binding and sequentially ordered dissociation	$[PP_i] = 15$ $K_{HX} = 7.7$, $K_{PRPP} = 66$ $K_{IMP} = 5.8$, $K_{PP_i} = 39$ $K_{iPRPP} = 25$, $K_{iIMP} = 40$ $K_{iPP_i} = 260$	 $f_{hprt1} = 1.1$ $f_{hprt2} = -0.89$ $f_{hprt,HX} = 0.48$	73 75
V_{aprt}	Michaelis–Menten	K_m (Ade) = 1.1–5.2 K_m (PRPP) = 6	f_{aprt6} = 0.52–0.84 $f_{aprt1} = 0.5$	76, 77
V_{aprt}	Competitive inhibition	$K_{Ade} = 0.9$, $K_{PRPP} = 5$ K_i = 7.5–30	$f_{aprt,AMP}$ = −0.76 to −0.96	76, 78
V_{polyam}	Michaelis–Menten	$K_m = 50$	$f_{polyam5} = 0.9$	79
V_{trans}	Michaelis–Menten	$K_m = 2$	$f_{trans5} = 0.33$	52, 80
V_{mat}	Michaelis–Menten	$K_m = 450$	$f_{mat,ATP} = 0.2$	52
V_{mat}	Uncompetitive inhibition with respect to methionine	K_i = 2–2.9	$f_{mat5} = -0.6$	52
V_{asuc}	Michaelis–Menten	K_m (IMP) = 30–700 K_m (GTP) = 30–130	f_{asuc2} = 0.23–0.87 $f_{asuc,GTP}$ = 0.09–0.30	81, 82
V_{asuc}	Competitive inhibition with respect to IMP	$K_i = 170$, K_m (IMP) = 37	$f_{asuc,AMP} = -0.24$	81
V_{asli}	Competitive inhibition	K_m (S-AMP) = 1.79 $K_i = 9.2$	$f_{asli3} = 0.99$ $f_{asli,AMP} = -0.95$	83
V_{impd}	Michaelis–Menten	K_m = 7–23	f_{impd2} = 0.07–0.19	84
V_{impd}	Competitive inhibition	$K_{iXMP} = 28$ $K_{iGMP} = 90$	$f_{impd7} = -0.09$ $f_{impd,GMP} = -0.03$	84
V_{gmps}	Michaelis–Menten	K_m (XMP) = 4.9 K_m (ATP) = 270	$f_{gmps7} = 0.16$ $f_{gmps,ATP} = 0.12$	85
V_{ampd}	Hill	K_m = 800–12 700 h = 0.9–2	$f_{ampd,AMP}$ = 0.4–1.2	86, 87
V_{ampd}	Competitive inhibition	K_i = 16 000 K_m (AMP) = 1000–10 000	f_{ampd18} = −0.07 to −0.08	87
V_{gmpr}	Michaelis–Menten	K_m (GMP) = 7.5	$f_{gmpr,GMP} = 0.23$	88
V_{arna} and V_{grna}	Michaelis–Menten	K_m (ATP) = 100 K_m (GTP) = 45	$f_{rnap,ATP} = 0.05$ $f_{rnap,GTP} = 0.13$	89
V_{adna} and V_{gdna}	Michaelis–Menten	K_m (dATP) = 3 K_m (dGTP) = 1.2	$f_{dnap,dATP} = 0.42$ $f_{dnap,dGTP} = 0.33$	90
V_{inuc}	Michaelis–Menten	K_m = 100–600	f_{inuc2} = 0.5–0.9	91
V_{gnuc}	Michaelis–Menten	$K_m = 700$	$f_{gnuc,GMP} = 0.9$	92
V_{adrnr}	Michaelis–Menten	K_m (ADP) = 40	$f_{adrnr,ADP} = 0.1$	93
V_{gdrnr}	Michaelis–Menten	K_m (GDP) = 50	$f_{gdrnr,GDP} = 0.4$	93
V_{dgnuc}	Michaelis–Menten	K_m (dGMP) = 3300	$f_{dgnuc,dGMP} = 1$	94
V_{ada}	Michaelis–Menten	K_m (Ado) = 17–100	$f_{ada,Ado}$ = 0.95–0.99	47, 55, 95
V_{dada}	Michaelis–Menten	K_m (dAdo) = 37–40	$f_{dada,dAdo} = 1$	95
V_{gua}	Michaelis–Menten	K_m (Gua) = 0.56	$f_{gua,Gua} = 0.5$	45
V_{hxd}	Michaelis–Menten	K_m (HX) = 12–14	$f_{hxd,HX} = 0.65$	96
V_{xd}	Michaelis–Menten	K_m (Xa) = 3–15.5	f_{xd14} = 0.37–0.75	97

states, and an assessment of its dynamic responses. These features are discussed in the following sections.

Validation of necessary conditions for model performance: steady-state stability and robustness

A basic feature for any model representing a normal physiological system is steady-state stability, unless oscillations play a specific role in the system, which is not the case for our target pathway. In order to test the stability of our model, the eigenvalues of the system at the physiological steady states were computed. Table 10 shows that all real parts are negative, which confirms that this steady state is locally stable, and that the system will return to it after small perturbations in any of the system variables.

As a second test for model performance, we use the sensitivities to changes in kinetic order parameters. High sensitivity is

Table 9 Estimated GMA kinetic orders, using methods 2 and 3

Units for concentrations are μM.

Reaction	Metabolite concentration	Change in flux rate (%)	Estimations	Reference	Method
V_{prpps}	[PRPP] = 1000	−19	$f_{prpps1} = -0.03$		
	[AMP] = 1000	−53	$f_{prpps,AMP} = -0.1$		
	[ADP] = 1000	−92	$f_{prps,ADP} = -0.36$	71	2
	[GMP] = 1000	−3	$f_{prpps,GMP} = -0.004$		
	[GDP] = 1000	−24	$f_{prpps,GDP} = -0.04$		
V_{den}	[IMP] = 5000	−41	$f_{den2} = -0.06$		
	[AMP] = 5000	−76	$f_{den,AMP} = -0.17$		
	[ADP] = 5000	−40	$f_{den,ADP} = -0.06$		
	[ATP] = 5000	−21	$f_{den,ATP} = -0.028$	21	2
	[GMP] = 5000	−70	$f_{den,GMP} = -0.14$		
	[GDP] = 5000	−40	$f_{den,GDP} = -0.06$		
	[GTP] = 5000	−13	$f_{den,GTP} = -0.016$		
V_{den}	$[P_i] = 25000$	From 38 to 17	$f_{den18} = -0.08$	98	3
V_{asuc}	$[P_i] = 2000$	−20	$f_{asuc18} = -0.05$	99	2
	$[P_i] = 20000$	−59			
V_{ampd}	[GTP] = 1000	From 25 to 20	$f_{ampd,GTP} = -0.03$	86	3
V_{gmpr}	[IMP] = 33	−30	$f_{gmpr2} = -0.1$		
	[IMP] = 330	−70	$f_{gmpr2} = -0.2$		
	[XMP] = 33	−93	$f_{gmpr7} = -0.76$	100	2
	[AMP] = 33	−5	$f_{gmpr,AMP} = -0.01$		
	[ADP] = 33	−7	$f_{gmpr,ADP} = -0.02$		
	[ATP] = 33	−11	$f_{gmpr,ATP} = -0.04$		
V_{gmpr}	[GDP] = 2	+13	$f_{gmpr,GDP} = 0.18$	88	2
	[GTP] = 2	+22	$f_{gmpr,GTP} = 0.29$		
V_{inuc}	$[P_i] = 1000$	From 0.5 to 0.04	$f_{inuc18} = -0.36$	92	3
V_{gnuc}	$[P_i] = 1000$	From 0.034 to 0.003	$f_{gnuc18} = -0.34$	92	3
V_{adrnr}	[dATP] = 5	−50	$f_{adrnr,dATP} = -0.3$	93	2

Table 10 Eigenvalues of the model at the original operating point

Real part	Imaginary part
-5.08×10^{-2}	0
-2.89×10^{-3}	0
-1.38×10^{-4}	0
-1.24×10^{-3}	0
-1.62×10^{-2}	0
-4.95×10^{-2}	3.17×10^{-4} i
-4.95×10^{-2}	-3.17×10^{-4} i
−0.265	0
−0.244	0
−0.371	0
−0.616	0
−0.743	0
−1.491	0
−5.533	0
−3.63	0
−39.6	0

typically an indicator for unreasonable responses of the model [34]. The sensitivities of the model appear in Figure 1. It should be noted that they are represented as absolute, instead of positive or negative, values. The use of absolute values simplifies the discussion and is sufficient for our purposes, because the robustness of the steady state is independent of the sign of each sensitivity. Most of the 1088 parameter sensitivities represented in Figure 1 are lower than 1, indicating that the model steady state considered at the normal physiological values is robust, a property that is expected in the real system [34].

The relatively high sensitivity $S(X_{13},f_{\mathrm{prpps18}})$ of 11.3 indicates that a 1% increase in f_{prpps18} will lead to an increase in X_{13} of about 11%. This sensitivity represents the influence of the activation of PRPPS by P_i on the concentration of X_{13}. However, the amplification indicated by this sensitivity is not very significant, because X_{13} is merely a degradation product of purine metabolism, and fluctuations in its concentration are inconsequential. Similarly, the sensitivities associated with the concentrations of X_2, X_6, X_{13} and X_{14} are of secondary importance. These particular variables are not the central metabolites of the pathway, but precursors or degradation products of the nucleotides or deoxynucleotides.

The only other sensitivities with higher values are associated with RNA and DNA. One is the sensitivity of RNA with respect to f_{rnan11}, and the other one is the sensitivity of DNA with respect to f_{dnan12}; all other sensitivities with respect to f_{rnan11} and f_{dnan12} are close to 0.

In summary, it is important to note that parameter sensitivities are low, indicating that the steady state of the model is robust. Therefore relatively inaccurate estimates of kinetic parameters will not significantly affect the global behaviour of the system. Moreover, because the central metabolites of the pathway are characterized by low sensitivities with respect to all kinetic orders, they are expected not to change dramatically after small changes in external conditions, a fact that is expected to occur in well-adapted biological systems [34].

Logarithmic gains

Logarithmic gains indicate how a system responds if one of the independent variables is perturbed. Gain profiles for both fluxes and concentrations therefore provide a reliable characterization

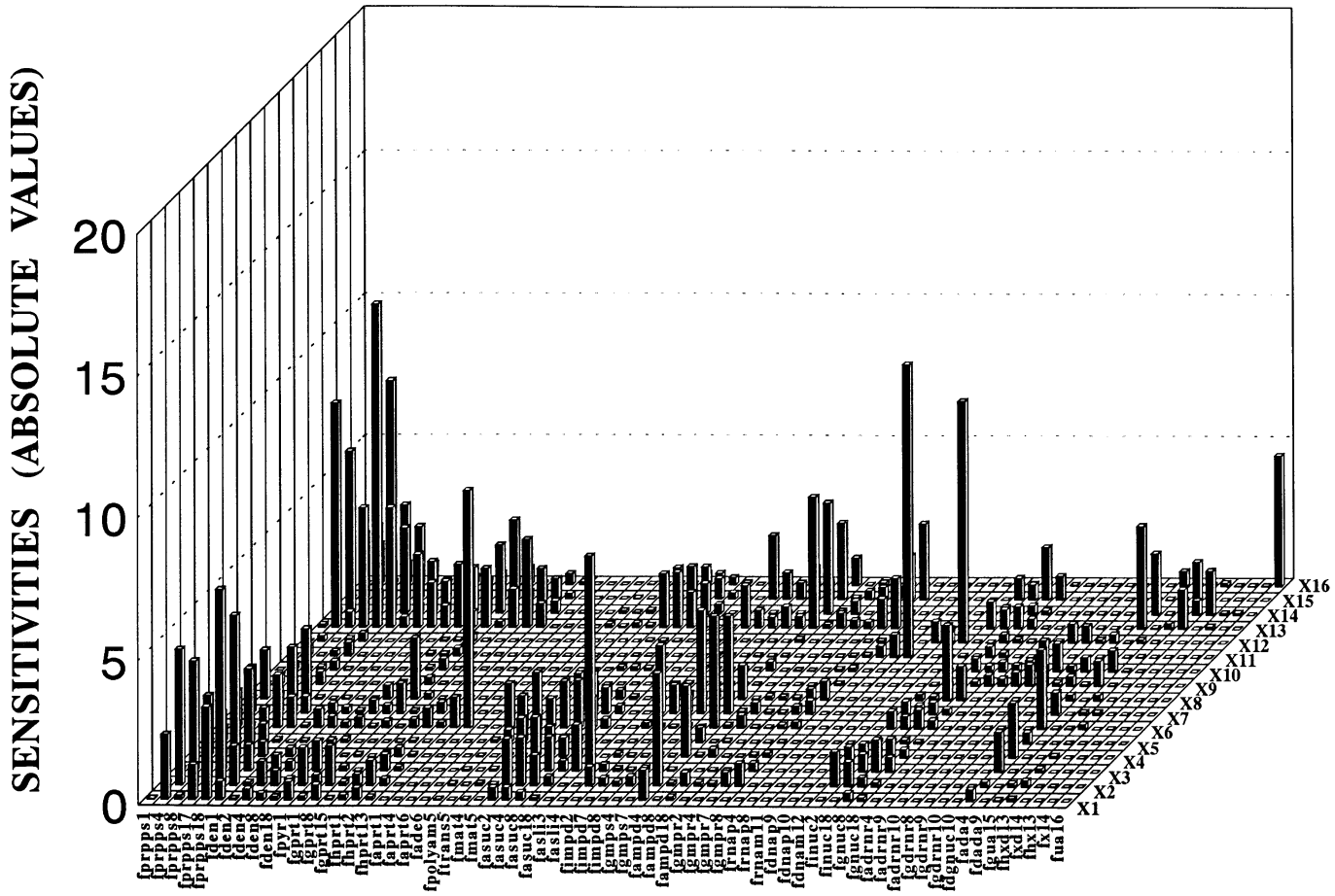

Figure 1 Absolute values of the sensitivities of concentrations with respect to kinetic orders

of the steady state for a given pathway. Gain profiles for our model are shown in Figures 2 and 3.

Biochemists generally have some information about those enzymes that have the greatest effect on the pathway. This information may derive from mutations that lead to altered enzymes and resultant disorders of purine metabolism or from known effectors of these enzymes. All available information about the enzymes of purine metabolism seems to be consistent with the results of our gain analysis (Figures 2 and 3). Enzymes with relatively high logarithmic gains, primarily PRPPS, HGPRT, IMPD and AMPD, are all known to be important in the regulation of purine metabolism, and inhibitors of these enzymes are often used for therapeutical purposes.

Although these enzymes have higher logarithmic gains than others, the results presented in Figures 2 and 3 show that the control of the pathway is widely distributed among the independent variables. The enzymes RNAP, RNAN, DNAP and DNAN are important only for the control of RNA and DNA and their synthesis or degradation, but have little effect on other variables of the model.

Some fluxes of the pathway are not catalysed by a single enzyme ($v_{pyr}, v_{ade}, v_{hx}, v_x$ and v_{ua}). In these cases, the independent variable in Figures 2 and 3 reflects a combination of enzymes. In some cases, two fluxes are equivalent at steady state ($v_{asuc} = v_{asli}$, $v_{impd} = v_{gmps}$ and $v_{xd} = v_{ua}$), and in other cases the kinetics of one flux is proportional to the kinetics of another flux. An example of the latter situation is the proportionality between the fluxes catalysed by DNAP and DNAN and RNAP and RNAN. In both cases, the logarithmic flux gains are the same for both fluxes, and one row of logarithmic gains is sufficient in Figure 3.

In some cases, the position of an enzyme within a pathway can significantly affect its influence on other fluxes and concentrations. In particular, it has been shown with mathematical rigour (R. Curto, E. O. Voit, A. Sorribas and M. Cascante, unpublished work), that, if the first step of a linear pathway is unmodified, subsequent steps can be lumped into a single step, and the kinetic properties of the pathway are determined by the kinetics of the first step. A case in point is the pathway consisting of the two reactions v_{asuc} and v_{asli}. The pathway is linear and the enzyme of the first reaction, ASUC, is unmodified. Therefore the enzyme ASLI, catalysing the second step, does not exert control over any other flux in the entire system. The situation is different in the case of v_{impd} and v_{gmps}. Here, GMPS exhibits some logarithmic flux gains that are not zero, because in the linear pathway of v_{impd} and v_{gmps} the first flux (v_{impd}) is affected directly by one of the variables of the pathway (XMP), and this constitutes the differences between this case and the case of v_{asuc}, which is not affected by S-AMP.

As is to be expected for a biochemical pathway in which fluxes are homogeneous functions of enzyme concentrations, and as a consequence of the mathematical representation selected for our model, the summation property proposed in MCT is satisfied for

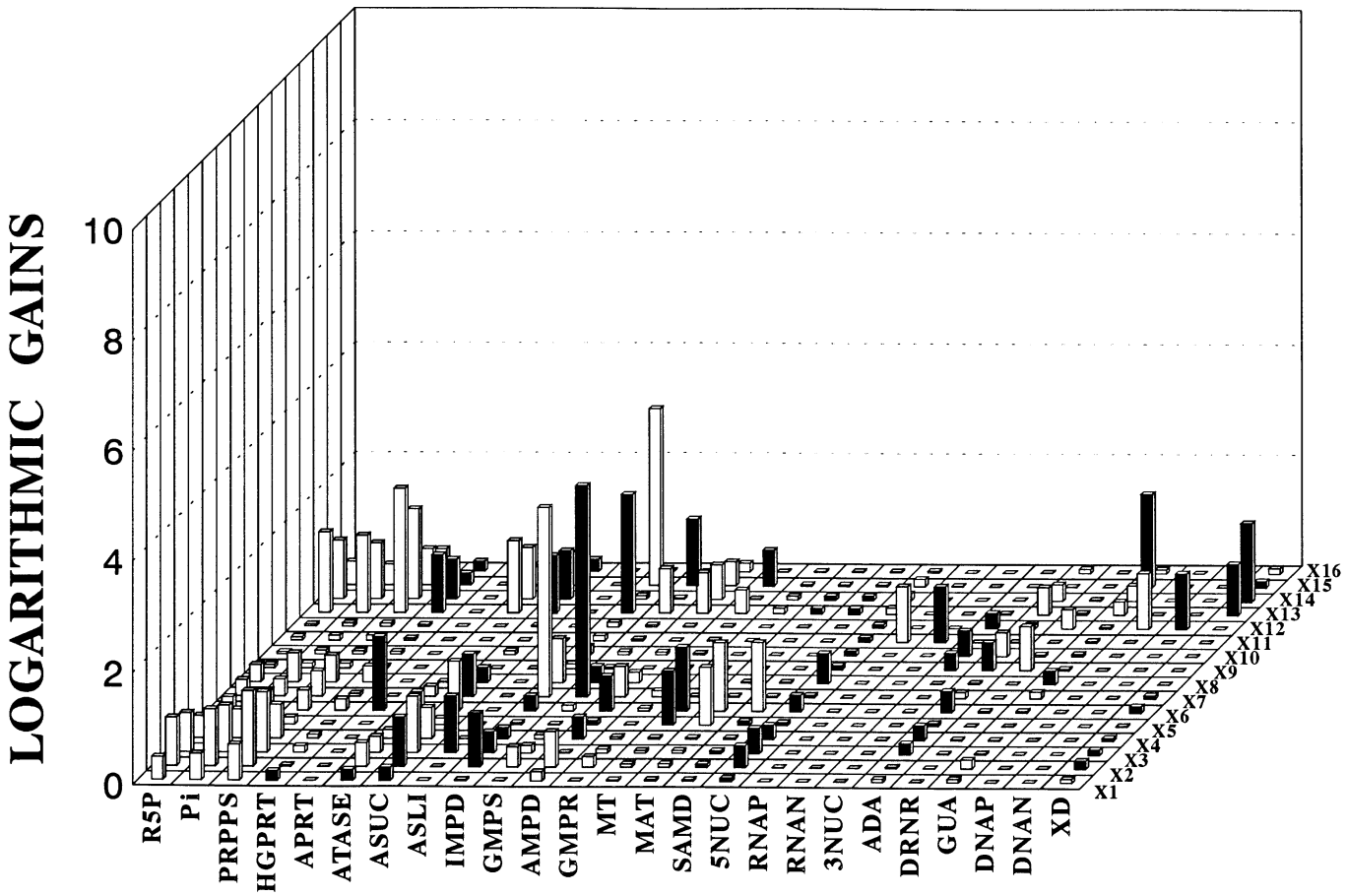

Figure 2 Logarithmic concentration gains for all relevant components of the pathway

Positive values are represented by open bars and negative values by solid bars.

both the individual flux rates and the metabolite concentrations. This property asserts

$$\sum_{i=1}^{l} C_{E_i}^{J} = 1 \quad \text{and} \quad \sum_{i=1}^{l} C_{E_i}^{X} = 0$$

where l is the total number of enzymes in the pathway, J is a flux of interest and X is one of the metabolite concentrations of the pathway [104,105].

Consistency of the model with experimental and clinical data

The analysis of the local stability of a model and the characterization of its sensitivities are crucial elements of any systems analysis. However, the fact that a system is stable and robust alone is only one necessary condition of validity. Maybe more important is whether the model reflects or predicts reality. This question is discussed below with a comparison of experimental or clinical findings with model results.

Constancy of adenine and guanine nucleotide pools

It is extensively documented in the literature that these pools remain almost constant under very different conditions [14] (see also [106]). To test whether our model accurately predicts this observation, we analysed the dynamic behaviour of the adenylates and guanylates after simulating the infusion or depletion of other system variables by the same absolute amount (100 μM increase or decrease on each variable). Table 11 shows the maximum or minimum values that X_4 and X_8 reached during the transition from the perturbed state back to the original steady state (2500 and 400 μM respectively), which the system always approached after some time. We simulated absolute instead of relative changes in each variable of the pathway because this corresponds to the same addition or subtraction or purine rings at different points of the network.

The results of these simulations demonstrate that temporary changes in DNA, Xa or UA do not yield appreciable alterations in the nucleotide pools. The injection or depletion of any of the other variables is buffered by the pathway, and it is evident that the adenylate and guanylate nucleotide pools are rather insensitive even to large changes in the other variables of the model, which is consistent with clinical findings in man.

Relatively larger changes in adenylates are observed as a consequence of initial changes in S-AMP. This is not surprising because S-AMP and the adenylates are part of a closed pathway, and S-AMP molecules have no choice other than to enter the adenylate pool. Noticeable changes are also produced by increases in SAM and Ade. Again, this fact is reported in the literature as an exception from the otherwise well-known unresponsiveness of adenylates (see under Incorporation of Ade and Gua below for more details). Apart from these variables, only temporary

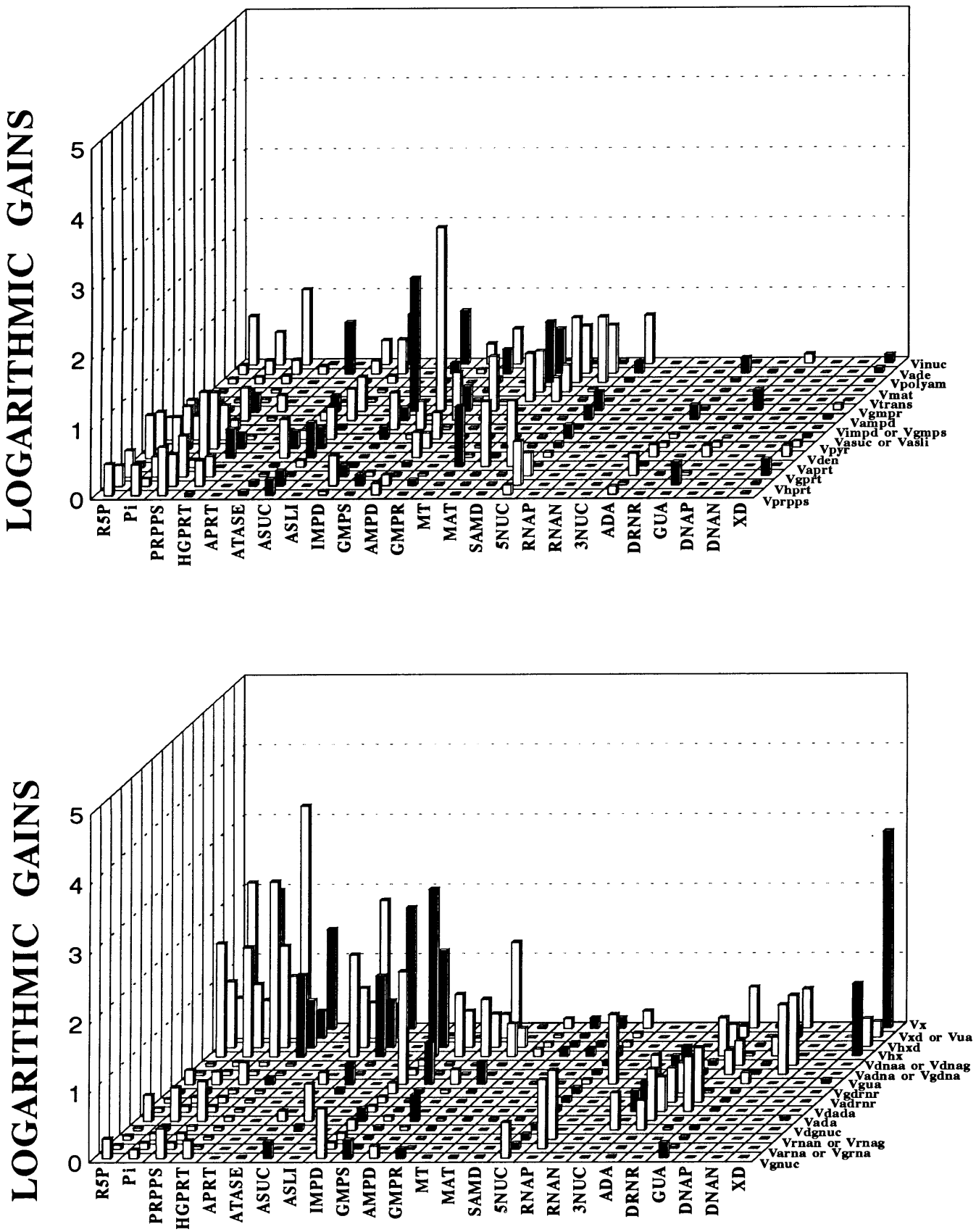

Figure 3 Logarithmic flux gains for all relevant components of the pathway

Positive values are represented by open bars and negative values by solid bars. The results are presented in two panels because of the large number of fluxes associated with purine metabolism.

Table 11 Maximum and minimum values reached by X_4 and X_8 in response to temporarily increasing or decreasing dependent variables

The concentrations at the physiological operating point are 2500 μM for adenylates (X_4) and 400 μM for guanylates (X_8). The variables X_{12}, X_{14} and X_{16} do not appear because adenylates and guanylates are not responsive to changes in these variables.

Variable name	Metabolite	Normal concentration (μm)	Externally set concentration (μM)	Transitional extreme value of adenylates (X_4) (μM)	Transitional extreme value of guanylates (X_8) (μM)
X_1	PRPP	5	105	2504 (max)	405 (max)
X_2	IMP	100	200	2536 (max)	401 (max)
X_2	IMP	100	1	2454 (min)	400
X_3	S-AMP	0.2	100.2	2595 (max)	397 (min)
X_5	SAM	4	104	2589 (max)	401 (max)
X_6	Ade	1	101	2591 (max)	394 (min)
X_7	XMP	25	125	2416 (min)	425 (max)
X_9	dAMP pool	6	106	2524 (max)	399 (min)
X_{10}	dGMP pool	3	103	2402 (min)	410 (max)
X_{11}	RNA	28600	28700	2514 (max)	409 (max)
X_{11}	RNA	28600	28500	2478 (min)	393 (min)
X_{13}	HX pool	10	110	2515 (max)	399 (min)
X_{15}	Gua	5	105	2432 (min)	417 (max)

changes in XMP and the deoxyguanylates affect the nucleotide pools appreciably.

Effects of hypoxanthine

Studying human bone marrow cells, King et al. [15] observed that a 100-fold increase in HX causes the rate v_{den} to decrease to a minimum of 19 % of its initial value (0.45 μmol/min per body weight). To test this response, we increased the initial value of HX by 100-fold. During the subsequent response phase, v_{den} reached a minimum value of 0.7 μmol/min per body weight, which reflects King's observation quite well.

Incorporation of Ade and Gua

Observations in human platelets [16], human muscle [17], Swis3T3 cells [18] and xanthinuric patients [19] suggest that the incorporation of Ade into adenylates is more significant than the incorporation of Gua into guanylates. The sixth and last rows of Table 11 demonstrate the strong response of adenylates after the addition of Ade and the weak response of guanylates after the addition of Gua, again suggesting consistency between model and experimental reports.

Inhibition of AMPD

A disorder has been reported in the literature in which the enzyme AMPD is resistant to inhibition by guanylates (f_{ampd4}) and P_i (f_{ampd18}). In humans, this resistance results in increases in UA and v_{xd} [20]. Setting the value of f_{ampd4} and f_{ampd18} equal to 0, the model reaches a new steady state, with a UA concentration of 117 instead of 100 μM and a v_{xd} of 3.24 instead of 2.3 μmol/min per body weight. Numerical values of [UA] and v_{xd} in patients with this disorder are not reported in [20], and we can only state that there is qualitative agreement between model results and clinical data.

Table 12 Clinically observed and simulated concentrations in subjects with PRPPS superactivity

For this simulation, the rate constant for PRPPS was changed from 0.9 to 1.8. The HX concentration has been calculated as 7/10 of X_{13}, because X_{13} also includes Ino and dIno, which are in equilibrium with HX.

	[UA] (μM)	[Xa] (μM)	[HX] (μM)	v_{den} (μmol/min per body weight)	[PRPP] (μM)
Control values	100	5	7.0	2.39	5.0
PRPPS superactivity simulation	131	15	28.7	4.70	7.8
Patients with PRPPS superactivity	300	10	21.0	8.55	21.0

PRPPS activity

Numerous reports have described the strong effect of increases in PRPPS activity on purine metabolism. In human subjects, increased PRPPS activity results in high concentrations of PRPP and UA, and in an increased flux v_{den} [21]. In patients with 200 % activity of this enzyme, PRPP increased from 270 to 520 % [107], and, in two other patients with the same disorder, HX, Xa and UA increased to 300, 200 and 300 % respectively [60]. Table 12 shows the concentrations at the operating point, simulated concentrations for a system with 200 % activity in PRPPS and clinically observed values in patients with PRPPS superactivity. The simulation results are in qualitative agreement with the clinical data.

HGPRT deficiency

Deficiencies in HGPRT can lead to dramatic changes in human purine metabolism. Many of these have been characterized in the literature; they are compared with model results in the following. In particular, HGPRT deficiency has been reported to result in: (i) a 3- or 4-fold increase in v_{den} in rats [22] and a 20-fold increase in v_{den} in humans [23]; (ii) increases in the concentration of HX from 6.9 to 50 μM in humans [29]; (iii) increases in the concentration of Xa from 5 to 15 μM in humans [29]; (iv) increases in the excretion of Xa and HX to about 9-fold the normal value in humans [29]; (v) increases in UA concentration from 100 to 150 μM in humans [25]; (vi) increases in UA excretion from 2.3 to values between 7 and 14 μmol/min per body weight [24].

For comparison, we implemented a 1 % HGPRT activity, thus simulating a rather severe deficiency. The resultant steady-state values are given in Table 13. The control values in this Table correspond to values measured in healthy subjects and thus to values of the original model at the operating point. The predictions of the model reflect the clinically measured values in HGPRT-deficient patients rather well.

APRT deficiency

Deficiencies in APRT are almost asymptomatic, except that the excretion of adenine metabolites (Ade, 8-hydroxyadenine and

Table 13 Clinically observed and simulated concentrations in HGPRT-deficient patients

Simulation results were obtained for 1% HGPRT activity. The HX concentration has been calculated as 7/10 of X_{13}, because X_{13} also includes Ino and dIno, which are in equilibrium with HX.

	[UA] (μM)	[Xa] (μM)	[HX] (μM)	V_{den} (μmol/min per body weight)	V_{ua} (μmol/min per body weight)	V_x (μmol/min per body weight)	V_{hx} (μmol/min per body weight)
Control values	100	5	7	2.39	2.30	0.03	0.05
HGPRT deficiency simulation	146	22	49	6.31	5.25	0.60	0.44
Patients with HGPRT deficiency	150	15	50	40.00	10.00	0.27	0.45

Table 14 Clinically observed and simulated concentrations in XD-deficient patients

Simulation results were obtained for 1% XD activity. The HX concentration has been calculated as 7/10 of X_{13}, because X_{13} also includes Ino and dIno, which are in equilibrium with HX.

	[UA] (μM)	[Xa] (μM)	[HX] (μM)	V_{ua} (μmol/min per body weight)	V_x (μmol/min per body weight)	V_{hx} (μmol/min per body weight)	Xa turnover (μmol/min per body weight)	UA turnover (μmol/min per body weight)
Control values	100	5	7	2.30	0.03	0.05	2.33	2.30
XD deficiency simulation	19	31	42	0.06	1.22	0.37	1.28	0.06
Patients with XD deficiency	1.6	15.8	12.3	0.045	1.155	0.28	1.20	0.045

2,8-dihydroxyadenine) is increased to values of about 0.5 μmol/min per body weight [26,27]. We simulated this deficiency by implementing a 1% APRT activity. As observed clinically, this change was almost inconsequential, and the steady state was essentially unaffected.The only exceptions were found to be the flux value for v_{ade} of 0.23 μmol/min per body weight, which is close to the value found in APRT-deficient patients, and an elevated adenine concentration of 310 μM. No information supporting or contradicting this considerable accumulation seems to be currently available in the literature.

Xanthinuria

Several metabolic alterations are associated with xanthinuria. They are reflected in the following clinical measurements: Xa turnover = 1.2, UA turnover = 0.045, $v_{hx} = 0.28$, $v_x = 1.155$ (the urinary excretion is only 1, and this flux includes other excretions that must be equivalent to Xa turnover minus UA turnover), $v_{ua} = 0.045$ μmol/min per body weight (the urinary excretion is only 0.02, and this flux includes other excretions equaling UA turnover), HX = 12.3, Xa = 15.8 and UA = 1.6 μM [28].

We implemented a 1% XD activity to simulate xanthinuria in humans. Values of the resulting steady state are given in Table 14. The predicted flux values are consistent with those in XD-deficient patients. The predicted concentrations are somewhat higher than those observed but qualitatively consistent with those in xanthinuric patients.

UA overproduction

In addition to the causes of elevated UA levels mentioned earlier in this section, there are a considerable number of conditions *in vivo* that cause overproduction of UA in humans. Examples include increases in PRPP, a surfeit of IMP [43,62] and increases in XD activity [108]. No quantitative clinical data for these conditions are available, but it is noted that our model qualitatively reproduces all these clinical observations over a vast range of changes in PRPP, IMP or XD activity (results not shown).

DISCUSSION

Mathematical models of biochemical systems offer an alternative to experimentation that allows the researcher to minimize cost and to test situations that are difficult or unethical in their implementation. They are also a prerequisite for a true understanding of the complexity of metabolic pathways [109]. Of course, before one can trust a mathematical model, it needs to be subjected to a battery of tests. There is never proof that a model is correct and, in fact, models are 'wrong' by design, since they simplify reality and ignore effects that could potentially be more significant than originally thought. Nonetheless, if mathematical analyses confirm the intrinsic validity and robustness of a model and if numerical simulations yield consistency with observed data, confidence in the model increases.

The model proposed in this paper was constructed from proven principles of systems analysis and estimated in its entirety from data found in the reviewed literature. The reliance on observed data and the structural robustness provided us with reasonable confidence about the validity of the model. The mathematical analyses of stability and various types of sensitivities corroborated this assessment.

Stability and robustness of the steady state are necessary, but by no means sufficient conditions for the quality of a model. It was therefore of great importance to simulate biochemical experiments and disorders of human purine metabolism that had been clinically documented. These simulations yielded good results, not only in terms of qualitative responses, but often quantitatively.

Beyond the comparisons with clinical and biochemical findings, the model analysis is interesting in two respects. First, the model integrates very different types of data, thereby allowing us to test

the consistency among different data sets and among data obtained under different conditions or from different organisms [110,111]. In this sense, the values obtained in Table 7, even though they merely constitute a collection of bibliographic data, are interesting in themselves because they elucidated the pattern of distribution of fluxes in human purine metabolism. Second, the model renders it possible to analyse questions about the design of the pathway [30]. Such design analyses explain the role of particular metabolites or modulators, as well as the rationale for the given pathway structure in comparison with other hypothetically possible structures [30].

Reliable mathematical models can be very attractive in the screening and analysis of 'what if' hypotheses. Such hypotheses can again address questions of design, but they can also be of great clinical and pharmaceutical interest. For instance, the establishment of logarithmic gain profiles can be a guide in the identification of processes that would be best suited for the drug treatment of a given disease. Enzymes with low gain factors are less likely candidates for efficacious manipulation than enzymes with high gains.

Reliable mathematical models can generate predictions not yet tested or even untestable in humans. Even if such predictions are only qualitative, they may provide clues about responses *in situ* and stimulate experimental investigation. For example, the prediction of significant adenosine accumulation in patients with APRT deficiency, to the best of our knowledge, has not been reported in the literature.

As an extension of the research presented here, we have recently used the model [8] to predict and explain neurological dysfunctions in patients with disorders of purine metabolism. This analysis sheds light on the biochemical mechanisms that result from some enzyme defects and classified primary and secondary causes of defects and disorders. Future research will address the specific effects of known and hypothetical drugs that interact with purine metabolism.

This work was funded by a Grant from Fondo de Investigaciones Sanitarias de la Seguridad Social (FISss 94/0860), and supported in part by a grant from The Upjohn Company. R.C. was funded as a Ph.D. student by CIRIT BQF92.

REFERENCES

1 Plunkett, W. and Saunders, P. P. (1994) in Anticancer Drugs: Antimetabolite Metabolism and Natural Anticancer Agents. Metabolism and Action of Purine Nucleoside Analogs, (Powis, G., ed.), pp. 95–137, Pergamon Press, Oxford
2 Hitchings, G. H. (1991) Adv. Exp. Med. Biol. **309A**, 1–6
3 Bottiglieri, T. and Hyland, K. (1994) Acta Neurol. Scand. **89**, 19–26
4 Peters, G. J. and Beijnen, J. H. (1994) Pharm. World Sci. **16**, 37–38
5 Franco, R. and Canela, E. I. (1984) Eur. J. Biochem. **144**, 305–315
6 Heinmets, F. (1989) Cell Biophys. **14**, 283–323
7 Bartel, T. and Holzhütter, H. (1990) Biochim. Biophys. Acta **1035**, 331–339
8 Curto, R. (1996) Ph.D Thesis, Universitat de Barcelona
9 Shiraishi, F. and Savageau, M. A. (1992) J. Biol. Chem. **267**, 22912–22918
10 Shiraishi, F. and Savageau, M. A. (1993) J. Biol. Chem. **268**, 16917–16928
11 Shiraishi, F. and Savageau, M. A. (1992) J. Biol. Chem. **267**, 22934–22943
12 Shiraishi, F. and Savageau, M. A. (1992) J. Biol. Chem. **267**, 22926–22933
13 Shiraishi, F. and Savageau, M. A. (1992) J. Biol. Chem. **267**, 22919–22925
14 Cory, J. G. (1988) in Bioquímica: Metabolismo de los Nucleótidos Purínicos y Pirimidínicos (Devlin, T. M., ed.), pp. 618–667, Reverte S. A., Barcelona
15 King, M. E., Honeysett, J. M. and Howell, S. B. (1983) J. Clin. Invest. **72**, 965–970
16 Jerushalmy, Z., Sperling, O., Pinkhas, H., Krinska, M. and Vries, A. (1973) Adv. Exp. Med. Biol. **41**, 159–162
17 Jacobs, A. E. M., Oosterhof, A. and Veerkamp, J. H. (1988) Biochim. Biophys. Acta **970**, 130–136
18 Ishijima, S., Kita, K., Kinoshita, N., Ishizuka, T., Suzuki, N. and Tatibana, M. (1988) J. Biochem, (Tokyo) **104**, 570–575
19 Ayvazian, J. H. and Skupp, S. (1965) J. Clin. Invest. **44**, 1248–1260
20 Van den Berghe, G. and Hers, H. G. (1980) Lancet **ii**, 1090
21 Holmes, E. W. (1981) Adv. Enzyme. Regul. **19**, 215–230
22 Zorefshani, E., Bromberg, Y., Brosh, S., Sidi, Y. and Sperling, O. (1993) J. Neurochem. **61**, 457–463
23 Edwards, N. L., Recker, D. and Fox, I. H. (1979) J. Clin. Invest. **63**, 922–930
24 Seegmiller, J. E. and Rosenbloom, F. M. (1967) Science **155**, 1682–1684
25 Fujimori, S., Tagaya, T., Yamaoka, N., Kamatani, N. and Akaoka, L. (1991) Adv. Exp. Med. Biol. **309B**, 101–104
26 Van Acker, K. J., Simonds, H. A., Potter, C. and Cameron, J. S. (1977) N. Engl. J. Med. **297**, 127–132
27 Van Acker, K. J. and Simonds, H. A. (1991) Adv. Exp. Med. Biol. **309B**, 91–94
28 Holmes, E. W. and Wyngaarden, J. B. (1980) in The Metabolic Basis of Inherited Disease. Hereditary Xanthinuria (Scriver, C. R., Beaudet, A. L., Sly, W. S. and Valle, D., eds.), pp. 1085–1094, McGraw-Hill, New York
29 Harkness, R. A. (1989) Adv. Exp. Med. Biol. **253A**, 159–163
30 Savageau, M. A. (1976) Biochemical Systems Analysis: A Study of Function and Design in Molecular Biology, Addison-Wesley, Reading, MA., London
31 Curto, R., Sorribas, A. and Cascante, M. (1995) Math. Biosci. **130**, 25–50
32 Voit, E. O., Irvine, D. H. and Savageau, M. A. (1991) The User's Guide to ESSYNS, Medical University of South Carolina Press, Charleston
33 Savageau, M. A. (1976) in Biochemical Systems Analysis. Nonlinear Systems Analysis (Savageau, M. A., ed.), pp. 118–130, Addison-Wesley, Reading, MA
34 Savageau, M. A. (1971) Nature (London) **229**, 542–544
35 Cascante, M., Curto, R. and Sorribas, A. (1995) J. Biol. Syst. **3**, 105–113
36 Wolfram, S. (1991) Mathematica. A System for Doing Mathematics by Computer, 2nd edn., Addison-Wesley Publishing Company, Reading, MA
37 Savageau, M. A. and Sorribas, A. (1989) J. Theor. Biol. **141**, 93–115
38 Sorribas, A., Curto, R. and Cascante, M. (1995) Math. Biosci. **130**, 71–84
39 Cascante, M., Curto, R. and Sorribas, A. (1995) Math. Biosci. **130**, 51–69
40 Cascante, M., Franco, R. and Canela, E. I. (1989) Math. Biosci. **94**, 271–288
41 Cascante, M., Franco, R. and Canela, E. I. (1989) Math. Biosci. **94**, 289–309
42 Ehlde, M. and Zacchi, G. (1995) Comp. Appl. Biosci. **11**, 201–207
43 Wyngaarden, J. B. and Kelley, W. N. (1983) in The Metabolic Basis of Inherited Disease. Gout (Stanbury, J. B., Wyngaarden, J. B., Fredrickson, D. S., Goldstein, J. L. and Brown, M. S., eds.), pp. 1043–1114, McGraw-Hill, New York
44 Kamatani, N., Kuroshima, S., Terai, C., Hakoda, M., Nishioka, K. and Mikanagi, K. (1989) Adv. Exp. Med. Biol. **253A**, 51–58
45 Giacomello, A. and Salerno, C. (1991) Adv. Exp. Med. Biol. **309B**, 253–256
46 Goodman, M. N. and Lowenstein, J. M. (1977) J. Biol. Chem. **252**, 5054–5060
47 Geiger, J. D. and Nagy, J. I. (1990) in Adenosine and Adenosine Receptors. Adenosine Deaminase and [^{3}H]Nitrobenzylthioinosine as Markers of Adenosine Metabolism and Transport in Central Purinergic Systems (Williams, M., ed.), pp. 255–288, The Humana Press, Clifton, NJ
48 Pillwein, K., Chiba, P., Knoflach, A., Czermak, B., Schuchter, K., Gersdorf, E., Ausserer, B., Murr, C., Goebl, R., Stockhammer, G., Maier, H. and Kostron, H. (1990) Cancer Res. **50**, 1576–1579
49 Grune, T., Siems, W. G., Gerber, G. and Uhlig, R. (1991) J. Chromatogr. **553**, 193–199
50 Tabucchi, A., Carlucci, F., Pagani, R., Ciccomascolo, F., Lopalco, L. and Siccard, A. (1991) Adv. Exp. Med. Biol. **309A**, 121–124
51 Barber, J. R., Morimoto, B. H., Brunauer, L. S. and Clarke, S. (1986) Biochim. Biophys. Acta **887**, 361–372
52 Oden, K. L. and Clarke, S. (1983) Biochemistry **22**, 2978–2986
53 Grune, T., Siems, W., Uhlig, R., Langen, P. and Gerber, G. (1991) Adv. Exp. Med. Biol. **309A**, 109–112
54 Morgan, G., Strobel, S., Montero, C., Duley, J. A., Davies, P. M. and Simmonds, H. A. (1991) Adv. Exp. Med. Biol. **309B**, 297–300
55 Kredich, N. M. and Hersfield, M. S. (1989) in The Metabolic Basis of Inherited Disease. Immunodeficiency Diseases Caused by Adenosine Deaminase Deficiency and Purine Nucleoside Phosphorylase Deficiency (Scriver, C. R., Beaudet, A. L., Sly, W. S. and Valle, D., eds.), pp. 1045–1075, McGraw-Hill, New York
56 Kunjara, S., Sochor, M., Greenbaum, A. L. and Mclean, P. (1993) Biochem. Med. Metab. Biol. **49**, 217–227
57 Albe, K. R. and Wright, B. E. (1994) J. Theor. Biol. **169**, 243–251
58 Stryer, L. (1988) in Bioquímica. DNA y RNA: Las Moléculas de la Herencia (Stryer, L., ed.), pp. 71–91, Reverté S. A., Barcelona
59 Siems, W. G., Grune, T., Schmidt, R., Uhlig, R., Gerber, G., Tikhonov, Y. V., Pimenov, A. M. and Toguzov, R. T. (1991) Adv. Exp. Med. Biol. **309A**, 113–116
60 Jimenez, M. L., Puig, J. G., Mateos, F. A., Ramos, T. H., Melian, J. S., Nieto, V. G. and Becker, M. A. (1989) Adv. Exp. Med. Biol. **253A**, 9–13
61 Bradford, M. J., Krakoff, I. H., Leeper, R. and Balis, M. E. (1968) J. Clin. Invest. **47**, 1325–1332
62 Palella, T. D. and Fox, I. H. (1989) in The Metabolic Basis of Inherited Disease. Hyperuricemia and Gout (Scriver, C. R., Beaudet, A. L., Sly, W. S. and Valle, D., eds.), pp. 965–1006, McGraw-Hill, New York
63 Traut, T. W., Ropp, P. A. and Poma, A. (1991) Adv. Exp. Med. Biol. **309B**, 177–180

64 Whelan, J. M. and Bagnara, A. S. (1979) Biochim. Biophys. Acta. **563**, 466–478
65 Page, T., Nyhan, W. L., Yu, A. L. and Yu, J. (1991) Adv. Exp. Med. Biol. **309B**, 345–348
66 Ayvazian, J. H. and Skupp, S. (1966) J. Clin. Invest. **45**, 1859–1864
67 Synder, F. F. and Henderson, J. F. (1973) J. Biol. Chem. **248**, 5899–5904
68 Hershfield, M. S. and Seegmiller, J. E. (1976) J. Biol. Chem. **251**, 7348–7354
69 Kather, H. (1990) J. Biol. Chem. **265**, 96–102
70 Horton, H. R., Moran, L. A., Ochs, R. S., Rawn, J. D. and Scrimgeour, K. G. (1993) in Principles of Biochemistry. Transcription and the Processing of RNA (Horton, H. R., Moran, L. A., Ochs, R. S., Rawn, J. D. and Scrimgeour, K. G., eds.), chapter 21, Prentice-Hall, Englewood Cliffs
71 Fox, I. H. and Kelley, W. N. (1972) J. Biol. Chem. **247**, 2126–2131
72 Fox, I. H. and Kelley, W. N. (1971) J. Biol. Chem. **246**, 5739–5748
73 Albe, K. R., Butler, M. H. and Wright, B. E. (1990) J. Theor. Biol. **143**, 163–195
74 Henderson, J. F., Brox, L. W., Kelley, W. N., Rosenbloom, F. M. and Seegmiller, J. E. (1968) J. Biol. Chem. **243**, 2514–2522
75 Giacommello, A. and Salerno, C. (1978) J. Biol. Chem. **253**, 6038–6044
76 Simmonds, H. A., Sahota, A. S. and Van Acker, K. J. (1989) in The Metabolic Basis of Inherited Disease. Adenine Phosphoribosyltransferase Deficiency and 2,8-Dihydroxyadenine Lithiasis (Scriver, C. R., Beaudet, A. L., Sly, W. S. and Valle, D., eds.), pp. 1029–1044, McGraw-Hill, New York
77 Holmsen, H. and Rozenberg, M. C. (1968) Biochim. Biophys. Acta **157**, 266–279
78 Hori, M. and Henderson, J. F. (1966) J. Biol. Chem. **241**, 3404–3408
79 Pegg, A. E. and Williams-Ashman, H. G. (1969) J. Biol. Chem. **244**, 682–693
80 Clarke, S. (1985) Annu. Rev. Biochem. **54**, 479–506
81 Van der Weyden, M. B. and Kelley, W. N. (1974) J. Biol. Chem. **249**, 7282–7289
82 Matsuda, Y., Ogawa, H., Fukutome, S., Shiraki, H. and Nakagawa, H. (1977) Biochem. Biophys. Res. Commun. **78**, 766–771
83 Stone, R. L., Zalkin, H. and Dixon, J. E. (1993) J. Biol. Chem. **268**, 19710–19716
84 Pugh, M. E. and Skibo, E. B. (1993) Comp. Biochem. Physiol. B **105**, 381–387
85 Page, T., Bakay, B. and Nyhan, W. L. (1984) Int. J. Biochem. **16**, 117–120
86 Nowak, G. and Kaletha, K. (1991) Biochem. Med. Metab. Biol. **46**, 263–266
87 Nowak, G. and Kaletha, K. (1992) Biochem. Med. Metab. Biol. **47**, 232–241
88 Spector, T., Jones, T. E. and Miller, R. L. (1979) J. Biol. Chem. **254**, 2308–2315
89 Ballard, P. L. and Williams-Ashman, H. G. (1966) J. Biol. Chem. **241**, 1602–1615
90 Fisher, P. A., Wang, T. S. and Korn, D. (1979) J. Biol. Chem. **254**, 6128–6137
91 Zimmermann, H. (1992) Biochem. J. **285**, 345–365
92 Itoh, R. (1981) Biochim. Biophys. Acta **657**, 402–410
93 Eriksson, S., Thelander, L. and Akerman, M. (1979) Biochemistry **18**, 2948–2952
94 Höglund, L. and Reichard, P. (1990) J. Biol. Chem. **265**, 6589–6595
95 Boyer, P. D. (1993) Biochim. Biophys. Acta **276**, 257–271
96 Strittmatter, C. F. (1965) J. Biol. Chem. **240**, 2557–2564
97 Bondy, P. K. and Rosenberg, L. E. (1974) Duncan's Diseases of Metabolism, Saunders, Philadelphia
98 Kovarsky, J., Evans, M. C. and Holmes, E. W. (1978) Can. J. Biochem. **56**, 334–338
99 Ogawa, H., Shiraki, H., Matsuda, Y., Kakiuchi, K. and Nakagawa, H. (1977) J. Biochem. (Tokyo) **81**, 859–869
100 Mackenzie, J. J. and Sorensen, L. B. (1973) Biochim. Biophys. Acta **327**, 282–294
101 de Verdier, C. H., Ericson, A., Niklasson, F. and Westman, M. (1977) Scand. J. Clin. Lab. Invest. **37**, 567–575
102 Lathem, W. and Rodnan, G. P. (1962) J. Clin. Invest. **41**, 1955–1963
103 Reference deleted
104 Kacser, H. and Burns, J. A. (1973) Symp. Soc. Exp. Biol. **27**, 65–104
105 Heinrich, R. and Rapoport, T. A. (1974) Eur. J. Biochem. **42**, 89–95
106 Galazzo, J. L. and Bailey, J. E. (1990) Enzyme Microb. Technol. **12**, 162–172
107 Becker, M. A., Puig, J. G., Mateos, F. A., Jimenez, M. L., Kim, M. and Simmonds, H. A. (1989) Adv. Exp. Med. Biol. **253A**, 15–22
108 Marcolongo, R., Marinello, E., Pompucci, G. and Pagani, R. (1974) Arthritis Rheum. **17**, 430–438
109 Stephanopoulos, G. and Sinskey, A. J. (1993) Trends Biotechnol. **11**, 392–396
110 Okamoto, M. and Savageau, M. A. (1984) Biochemistry **23**, 1701–1709
111 Okamoto, M. and Savageau, M. A. (1986) Biochemistry **25**, 1969–1975

Received 2 August 1996/4 February 1997; accepted 5 February 1997